Analysis of the Physical Properties and Molecular Modeling of Sec13: A WD Repeat Protein Involved in Vesicular Traffic†

Kumkum Saxena,‡ Chrysanthe Gaitatzes,§ Mary T. Walsh,|| Michael Eck,⊥ Eva J. Neer,*,‡ and Temple F. Smith§

Department of Medicine, Cardiovascular Division, Brigham and Women's Hospital and Harvard Medical School, Boston, Massachusetts 02115, Department of Pharmacology and Biomolecular Engineering Research Center, Boston University, Boston, Massachusetts, Departments of Biophysics and Biochemistry, Boston University School of Medicine, Boston, Massachusetts, and Children's Hospital and Harvard Medical School, Boston, Massachusetts

Received July 3, 1996; Revised Manuscript Received September 12, 1996⊗

ABSTRACT: WD repeat proteins are a family of proteins that contain a series of highly conserved internal repeat motifs, usually ending with WD (Trp-Asp). The G_β subunit of heterotrimeric guanine nucleotide binding protein is a member of this family, and its crystal structure has been recently solved at high resolution (Wall et al. (1995) *Cell 83*, 1047−1058; Sondek et al. (1996) *Nature 379*, 369−374). Based on the coordinates of G_β, we have constructed a model for the structure of Sec13, a 33 kDa WD repeat protein from *Saccharomyces cerevesiae* essential for vesicular traffic. The model has been tested using a combination of biophysical and biochemical methods. Sec13 was expressed in *Escherichia coli* as a hexa-His-tagged protein (H6Sec13) and purified to homogeneity. In contrast to some other WD repeat proteins that are unable to fold into monomeric structures when expressed in *E. coli*, H6Sec13 was soluble and monomeric in the absence of detergent. The far-UV circular dichroism (CD) spectra of H6Sec13 indicated less than 10% α-helix consistent with the model which predicts primarily β-sheets. H6Sec13 shows a cooperative and irreversible thermal denaturation curve consistent with a tightly packed structure. The CD spectrum shows an unusual positive ellipticity at 229 nm that was attributed to interactions of surface tryptophans since the 229 nm maximum could be abolished by modification of 6.3 ± 0.3 ($n = 3$) tryptophans (out of 15 total in the molecule) with *N*-bromosuccinimide. Our model predicts that three sets of tryptophans are clustered near the surface. As predicted by the model, purified H6Sec13 was completely resistant to trypsin digestion. The concordance of the model of Sec13 presented in this paper with the biochemical and biophysical studies suggests that this model can be useful as a guide to further experiments designed to elucidate the function of Sec13 in vesicular traffic.

WD repeat proteins are a family of proteins with very diverse cellular functions including regulation of signal transduction, pre-mRNA processing, gene transcription, cell cycle progression, development, vesicular traffic, and cytoskeleton assembly (Neer et al., 1994). Members of this family are made up of highly conserved repeating units called WD repeats. Each repeating unit consists of a core region of approximately 40 amino acids typically bracketed by GH (glycine-histidine) and WD (tryptophan-aspartate), and a variable region of 6−94 amino acids. This repeating unit was first recognized in the G_β subunit of heterotrimeric guanine nucleotide-binding proteins that transduce signals across the plasma membrane (Fong et al., 1986). G_β is made up of seven such repeating units plus an N-terminal extension and is dependent on the G_γ subunit for its correct folding (Schmidt & Neer, 1991). Very recently, two independent groups have determined the crystal structure of $G_{\beta\gamma}$ (Wall et al., 1995; Lambright et al., 1996; Sondek et al., 1996). G_β forms a propeller structure in which the seven blades of the propeller are formed by the seven WD repeats. Each propeller blade consists of a small four-stranded twisted β-sheet, the innermost β-strand being nearly parallel to the axis of the central tunnel. The β-propeller structure is not unique to G_β and has been observed in several non-WD repeat proteins such as galactose oxidase (Ito et al., 1994), hemopexin (Faber et al., 1995), methanol dehydrogenase (Xia et al., 1992), collagenase (Li et al., 1995), and methylamine dehydrogenase (Chen et al., 1992) (reviewed by Neer & Smith, 1996). The α-carbon atoms of the three inner strands of all the seven G_β WD repeats can be superimposed onto two of the non-WD repeat containing propeller structures (porcine collagenase and methylamine dehydrogenase) with 0.9−2.2 Å root mean square deviation (Neer & Smith, 1996). The similarity between a WD repeat propeller and a non-WD repeat propeller structure suggests that the other WD repeat proteins also fold into propeller structures.

Based on the crystal structure of G_β, we have created a model for the structure of another WD repeat protein, Sec13. Sec13 is a 33 kDa protein from *Saccharomyces cerevisiae* that is involved in vesicular transport (Pryer et al., 1993; Salama et al., 1993). Recently, Swaroop et al. (1994) have identified a human gene, Sec13R, that encodes a protein with

† This work was supported by National Institutes of Health grant GM36359 (to E.J.N.) and by Grant P41 LM05252 from the National Library of Medicine (to T.F.S.). The contents of this paper are solely the responsibility of the authors and do not necessarily represent the official views of the granting organizations.

* Please address correspondence to: Dr. Eva J. Neer, Cardiovascular Division, Brigham and Women's Hospital, 75 Francis St., Boston, Massachusetts 02115. 617-732-5866; 617-732-5132 (FAX).

‡ Brigham and Women's Hospital and Harvard Medical School.

§ Boston University.

|| Boston University School of Medicine.

⊥ Children's Hospital and Harvard Medical School.

⊗ Abstract published in *Advance ACS Abstracts,* November 15, 1996.

S0006-2960(96)01616-9 CCC: $12.00

53% identity and 70% similarity to the amino acid sequence of the yeast Sec13. Shaywitz et al. (1995) have shown that two reciprocal human/yeast fusion constructs, encoding the NH_2-terminal half of one protein and the COOH-terminal half of the other, can complement the secretion defect of a Sec13 mutant at 36 °C. The amino acid sequence deduced from the cDNA (Pryer et al., 1993) shows that Sec13 is made up of six WD repeats with minimal N- and C-terminal extensions. Thus, Sec13 allows one to study the properties of the repeats themselves without the confounding contribution of non-WD repeat sequences. Furthermore, Sec13 is soluble when expressed in *Escherichia coli* and can be purified in large quantities, making it suitable for studies of the physical properties of a WD repeat protein. Other WD repeat proteins such as G_β or RACK1, a protein that binds protein kinase C (Ron et al., 1994), are insoluble when synthesized in *E. coli* (unpublished data). In this paper, we describe a model for the structure of Sec13 and investigate its implications using a combination of physical and biochemical approaches.

MATERIALS AND METHODS

Cloning, Expression, and Purification of H6Sec13. The Sec13 cDNA (kindly provided by Dr. C. A. Kaiser, MIT) was excised at the *Bam*HI and *Sac*I sites, subcloned into the pQE-31 expression vector (QIAGEN), and expressed as a hexaHis-tagged protein (H6Sec13) in M15 cells. For small scale purification, overnight cultures of *E. coli* transformed with H6Sec13 recombinant pQE-31 vector were diluted 1:50 in 500 mL of fresh LB media (100 μg/mL ampicillin, 25 μg/mL kanamycin) and grown at 37 °C until the OD_{600} reached 0.7−0.8 before adding isoprenyl β-D-thiogalactopyranoside (IPTG) to 0.5 mM. After a further 3 h of growth, cells were pelleted and resuspended in 1/10th culture volume of buffer A (50 mM sodium phosphate, pH 8.0, 300 mM NaCl). Cells were lysed by freezing and thawing, followed by brief sonication on ice, and centrifugation at 10000*g* for 20 min. The supernatant (crude extract A, soluble fraction) was filtered through a 0.45 μm filter (Millipore, catalog no. SLHA0250S) and applied on a 2-mL column of Ni-NTA (nitrilotriacetic acid) resin (QIAGEN, catalog no. 30230) preequilibrated with buffer A at about 18 mL/h. The column was washed with buffer A until the OD_{280} of the flow-through was less than 0.01 (approximately 80 mL). The resin was further washed with buffer B (50 mM sodium phosphate, pH 6.0, 300 mM NaCl) until the OD_{280} was less than 0.01, followed by three column volumes of buffer A. H6Sec13 was eluted with a 20-mL linear gradient of 0−0.5 M imidazole in buffer B. Fractions of 0.5 mL each were collected, and aliquots were analyzed by SDS−PAGE on 13% polyacrylamide gels (Laemmli, 1970). The peak fractions containing H6Sec13 were pooled (∼18 mL), concentrated to 1.3 mL using Amicon (YM10 membranes, Amicon, catalog no., 13612), and applied on to an AcA34 column (1 × 100 cm) preequilibrated with 50 mM Tris-HCl buffer, pH 8.0, at a flow rate of ∼18 mL/h. Fractions of 1 mL were collected. For large scale purification (10 L) the procedure was essentially the same except that 5 mM β-mercaptoethanol, 3 mM benzamidine, and 1 mM phenylmethylsulfonyl fluoride (PMSF) were included in the buffers. The cell pellet from 10 L of IPTG-induced culture was suspended in 80 mL of sonication buffer. Cells were lysed by sonication on ice using a flat tip at full power followed by overnight centrifugation at 4 °C at 40 000 rpm in a Ti45 rotor. H6Sec13 was purified from the supernatant on a 2.5 × 6.8 cm Ni-NTA column at 4 °C. Ni-NTA purified H6Sec13 was further purified by FPLC on a Superdex-75 (1.6 × 60 cm) column preequilibrated with 50 mM Tris-HCl, pH 8.0, 150 mM NaCl, and 5 mM β-mercaptoethanol.

Trypsin Digestion. Purified H6Sec13 (20 μg) in 0.1 M sodium phosphate buffer, pH 7.0, was treated with 40 pmol of tosylphenylalanyl chloromethyl ketone-treated trypsin (Cooper Biomed) in 40 μL total reaction volume, for 10 or 30 min at 30 °C. For heat-denatured samples, H6Sec13 was heated at 95 °C for 20 min prior to trypsin treatment. The digestion was halted by the addition of Laemmli sample buffer immediately followed by boiling for 5 min. Fragments were analyzed by SDS−PAGE on a 13% gel followed by staining with Coomassie Blue (Laemmli, 1970).

Determination of Stokes Radius. H6Sec13 purified on Ni-NTA resin was applied to a 7-mL AcA34 column equilibrated with 50 mM Tris-HCl, pH 8.0, 5 mM dithiothreitol (DTT), and 2 mM benzamidine at a flow rate of 10 mL/h, at 4 °C. Internal markers of known Stokes radius, bovine serum albumin (BSA) (37 Å), ovalbumin (28 Å), carbonic anhydrase (23 Å), and lactalbumin (20 Å), were included in the sample. Fractions of 300 μL were collected (after collecting 1.5 mL separately), and aliquots of fractions were analyzed by SDS−PAGE followed by densitometry of the Coomassie Blue-stained bands. The Stokes radius was determined by comparison of the elution position of H6Sec13 with elution position of the added markers of known Stokes radius.

Circular Dichroism (CD). CD spectra of H6Sec13 were recorded on an AVIV 62DS CD spectropolarimeter (AVIV Associates, Inc., Lakewood, NJ) calibrated from 500 to 190 nm with *d*-10-camphorsulfonic acid (1 mg/mL in ethanol). Spectra were measured at temperatures from 5 to 95 °C with sample temperature maintained to within 0.05 °C by use of a thermoelectric temperature controller. Samples were examined in 0.1 cm cells at a concentration of protein, ≈8 μM, chosen to maintain the dynode voltage below 600 V in the wavelength region 250−200 nm. Protein concentration was determined using absorption at 280 nm and an extinction coefficient of 94 490 cm^{-1} L mol^{-1}. The extinction coefficient was calculated from the composition of the protein (Gill & von Hippel, 1989). The spectrum reported for each sample represents the average of five individual spectra for each preparation and has been corrected for baseline contribution due to buffer (50 mM Tris-HCl, pH 8.0). For thermal denaturation studies, measurements were made at fixed wavelengths (228.5 and 203.5 nm) and samples were discontinuously heated at 0.1−1 °C/min (with incubation for 1 min between temperature increments).

Molar ellipticity values $[\Theta]$ (deg·cm^2/dmol) = $[\Theta\text{-}(MRW)]/[(10)(lc)]$, where Θ represents the displacement from the baseline value × full range in degrees, MRW equals the mean residue weight of an amino acid, l is the path length of the cell in cm, and c equals the concentration of protein in g/mL. All reported spectra were normalized to molar ellipticity values in deg·cm^2/dmol.

For tryptophan modification of H6Sec13 by *N*-bromosuccinimide (NBS), samples were treated with 0.5 mM NBS in buffer C (0.1 M sodium phosphate buffer, pH 7.0) for 5 min and the spectra were immediately recorded.

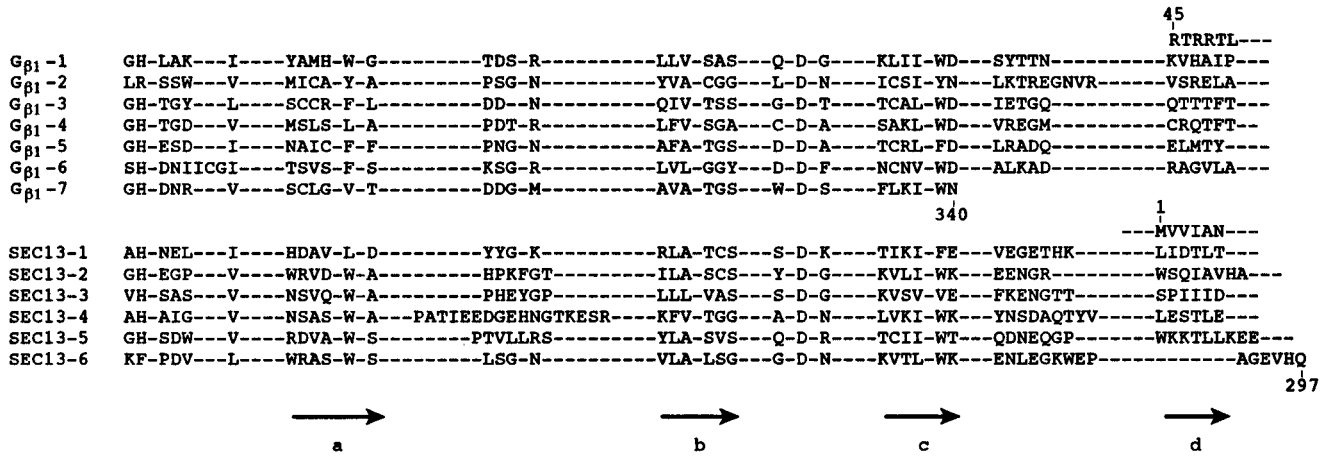

FIGURE 1: Sequence alignment of the WD repeats of $G_{\beta 1}$ and Sec13. Residues 45−340 of $G_{\beta 1}$ and the complete sequence (residues 1−297) of Sec13 were aligned. Regions representing the β-strands (strands a−d; see Figure 7A) are included below the aligned sequence.

UV Absorption. Modification of tryptophan residues of H6Sec13 by NBS was determined by recording the OD_{280} as a function of time on a Hewlett Packard 8452A diode array spectrophotometer. H6Sec13 (16−21 μM) in buffer C was treated with 0.5 mM NBS in the cuvette, and the OD_{280} was immediately measured as a function of time for 30 min. OD_{280} at zero time was obtained by the addition of equal volume of buffer instead of NBS. To measure any precipitation of H6Sec13 upon NBS treatment, OD_{600} was recorded as a function of time. The number of tryptophan residues modified were calculated using the following formula (Spande & Witkop, 1967):

$$\text{no. of tryptophans modified} = [(\Delta(\text{absorbance})_{280}) \times (1.31)]/[(5500)[\text{H6Sec13}]]$$

where $\Delta(\text{absorbance})_{280}$ is the difference in OD_{280} of NBS-treated and untreated samples, and [H6Sec13] is the molar concentration of H6Sec13.

Model Building. The three-dimensional model for yeast Sec13 was constructed by using homology extension modeling techniques, based on the crystallographically determined coordinates of the β subunit of heterotrimeric G proteins kindly provided by Dr. S. Sprang, Dallas, TX (Wall et al., 1995). G_β belongs to the β-propeller family of protein folding motifs. The propeller-like structure of G_β is formed by seven blade-like repeating units, each of which consists of four antiparallel β-strands.

Sec13 consists of six repeating units, homologous in sequence to the seven in G_β. Each of them was modeled as an antiparallel, four-stranded β-sheet. The sixth blade of G_β was excluded, since it contains a loop (SHDNIICGI) larger than any predicted in Sec13. To compensate for the difference in number of blades, the angle between subsequent blades was made approximately 9° wider than it is in the G_β seven-bladed structure. The energy of the resulting six-blade model was minimized in solution (structure solvated to 8 Å) using CHARMm version 23.1 (Brooks et al., 1983) (100 steps of Steepest Descents minimization, constraining the backbone residues). The alignment of Sec13 sequence to six out of the seven repeats of G_β is shown in Figure 1. Based on this alignment, the Sec13 β-strand backbone and oriented amino acid β-carbons were positioned in the G_β equivalent positions, resulting in an initial core model framework structure. Using this framework and the molecular modeling software package QUANTA version 4.1 (copyright MSI Inc.), we carried out assignments for the side chains. For model building of the loops, we substituted and inserted or deleted residues appropriately in the homologous G_β loops and used the "Regularize Region" option of QUANTA to assign coordinates for backbone and side chain atoms. This model structure was refined through energy minimization without any constraints (2000 steps of minimization using the adopted-basis Newton-Raphson (ABNR) algorithm, as implemented by CHARMm). It was subsequently heated from 0 to 2000 K in a molecular dynamics simulation with a time step of 0.001 ps, and then subjected to equilibration at 2000 K. Finally, the model was cooled down to 300 K, and was further refined by 2000 steps of ABNR unconstrained energy minimization. Comparison of model side chain contacts within each blade with those most consistently seen in the G_β were checked. Side chains of residues that appeared to make unfavorable or atypical contacts were placed in alternative positions maximizing the similarity to the contacts in G_β, with the use of SCULPT (Surles, 1992), and unconstrained minimization was subsequently repeated a final time.

RESULTS

Expression and Purification of H6Sec13. To facilitate the purification of Sec13 from *E. coli*, we created a fusion protein H6Sec13, containing an additional amino-terminal stretch of six histidines. The hexa-His tag binds very strongly to Ni-NTA resin and therefore permits purification of hexa-His-tagged proteins from less than 1% to greater than 95% homogeneity in a single step (Janknecht et al., 1991). Figure 2A shows the expression of H6Sec13 in *E. coli*. Under nondenaturing conditions, about 40−50% of the expressed H6Sec13 can be released as a soluble protein with an apparent molecular weight of 33 kDa (lane 3), and the rest goes into the particulate fraction (lane 4, Figure 2A). Purification of H6Sec13 from the soluble fraction on Ni-NTA resin resulted in a greater than 90-fold purification (lanes 1−3, Figure 2B). The final gel filtration chromatography removed the few contaminating proteins that eluted from Ni-NTA resin (lane 4, Figure 2B). Small scale purification of H6Sec13 from 500 mL of culture yielded a maximum of 2 mg of protein/L of culture. Scaling up the purification protocol to 10 L of starting culture greatly improved the efficiency of purification to give 8 mg/L of purified H6Sec13.

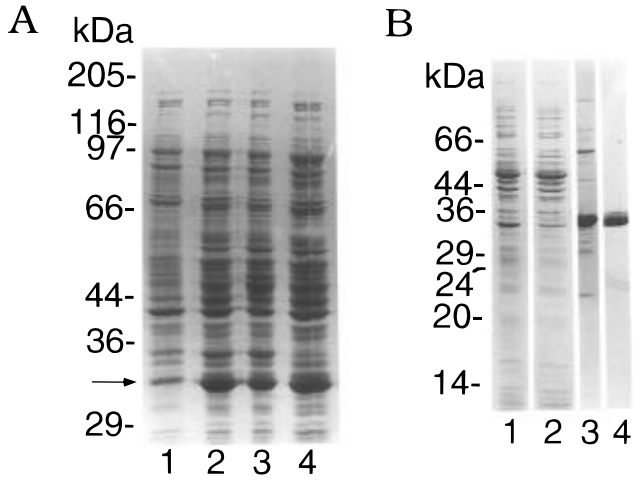

FIGURE 2: (A) Expression of H6Sec13 in *E. coli*. The methods are described in detail in the text. SDS−PAGE analysis of H6Sec13 in uninduced cells (lane 1), induced cells (lane 2), soluble fraction (lane 3), and particulate fraction (lane 4). (B) Purification of H6Sec13. SDS−PAGE analysis of the starting material (soluble fraction of H6Sec13, lane 1); flow through from Ni-NTA resin (lane 2); effluent from Ni-NTA resin (lane 3); and AcA34 purified H6sec13 following purification on Ni-NTA resin (lane 4).

In all of the preparations, a minor band (∼34 kDa) was observed which increased on heating and on storage at 4 °C. The presence of DTT or β-mercaptoethanol in the buffers did not prevent the formation of this band. The source of this band is unknown, but it seems to be a product of an internal modification of H6Sec13. This modification was not due to the six histidines present at the N-terminus of H6Sec13 since it is also observed in Sec13 without the hexahistidine tag translated *in vitro* (data not shown).

Determination of Stokes Radius. In vitro translated H6Sec13 folds into a globular monomeric protein (Garcia-Higuera et al., 1996). Proteins that fold well in the *in vitro* translation system do not necessarily fold into monomeric globular protein when expressed in *E. coli*. For example, most of RACK1, a WD repeat protein that binds protein kinase C (Ron et al., 1994), folds into a monomeric globular protein when translated *in vitro* or when purified from rat brain but aggregates when expressed in *E. coli* (unpublished data). In order to verify that H6Sec13 folded into a globular, monomeric protein purified H6Sec13 was analyzed by gel filtration chromatography (Figure 3). H6Sec13 has an apparent Stokes radius of 26.3 ± 1.7 Å ($n = 3$) similar to that of *in vitro* translated Sec13 which has a Stokes radius of 26.0 ± 0.3 Å ($n = 3$). The sedimentation coefficient of Sec13 translated *in vitro* in a rabbit reticulocyte lysate is 3.9 ± 0.2 S, giving a hydrodynamically calculated molecular weight of 33 000. The frictional ratio (f/f_0) of Sec13 is 1.22, indicating it is a globular, symmetric protein (Garcia-Higuera et al., 1996). The agreement of the Stokes radius determined for H6Sec13 synthesized in *E. coli* with that of Sec13 translated in rabbit reticulocyte lysate shows that the presence of six additional histidine residues at the N-terminus does not affect the folding of Sec13.

Trypsin Digestion. Further evidence that H6Sec13 forms a compact structure is its resistance to cleavage by trypsin despite 28 potential trypsin cleavage sites (lanes 2 and 3, Figure 4). In contrast, heat-denatured H6Sec13 is completely degraded into small pieces when treated with trypsin (lanes 4 and 5, Figure 4).

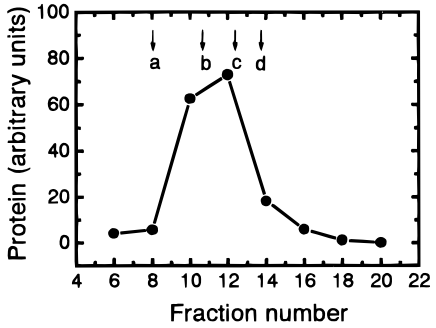

FIGURE 3: Determination of Stokes radius: H6Sec13 purified on Ni-NTA was applied to a 0.7 × 18 cm (7-mL) AcA34 column equilibrated with 50 mM Tris-HCl, pH 8.0, 5 mM DTT, and 2 mM benzamidine and eluted at a flow rate of 10 mL/h at 4 °C. Internal markers were included in the sample. Their elution positions are indicated by arrows: a, BSA (37 Å); b, ovalbumin (28 Å); c, carbonic anhydrase (23 Å); and d, lactalbumin (20 Å). Fractions of 300 μL were collected (after collecting 1.5 mL separately) and aliquots were analyzed by SDS−PAGE followed by densitometry of the Coommassie Blue-stained bands ($S_{20,w} = 26.3 \pm 1.7$ ($n = 3$)). The peak position was calculated from the half-width position at half-height.

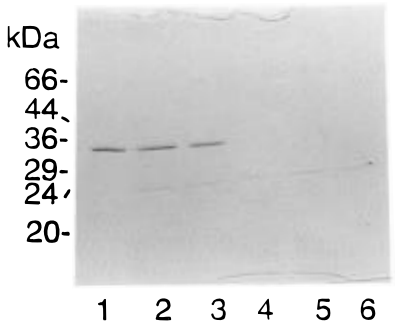

FIGURE 4: SDS−PAGE analysis of purified H6Sec13 cleaved with trypsin. Lane 1, uncut H6Sec13; lanes 2 and 3, H6Sec13 treated with 1 μM trypsin for 10 and 30 min, respectively; lanes 4 and 5, heat-denatured H6Sec13 treated with 1 μM trypsin for 10 and 30 min, respectively; and lane 6, trypsin.

Circular Dichroism and UV Absorption. The overall percentage of α-helix calculated from the CD spectrum was estimated to be less than 10% calculated from the molar ellipticity at 208 nm (Greenfield & Fasman, 1969). The far-UV−CD spectrum of H6Sec13 at room temperature, shows a pronounced maximum at 229 nm (Figure 5A). In other proteins, this positive molar ellipticity at around 230 nm has been ascribed to the presence of disulfide bonds or interactions between aromatic residues, such as tryptophans, phenylalanines, and tyrosines (Hider et al., 1988; Woody, 1978). H6Sec13 has 15 tryptophans and only three cysteines. In order to determine the source of the positive ellipticity of H6Sec13 at 229 nm, the tryptophan residues were modified with NBS. Figure 5A shows the CD spectra of H6Sec13 before and after treatment with NBS. Treatment with NBS completely abolishes the maximum at 229 nm, indicating that interactions between tryptophan residues may be responsible for the 229 nm maximum.

Reaction of NBS with the tryptophan residues of H6Sec13 was found to be very fast as shown in Figure 5B. Upon the addition of NBS, a sharp decrease in OD_{280} is observed as a function of time. Most of the reaction is completed within the first minute. The light scattering effect due to any precipitation of H6Sec13 was measured by monitoring the

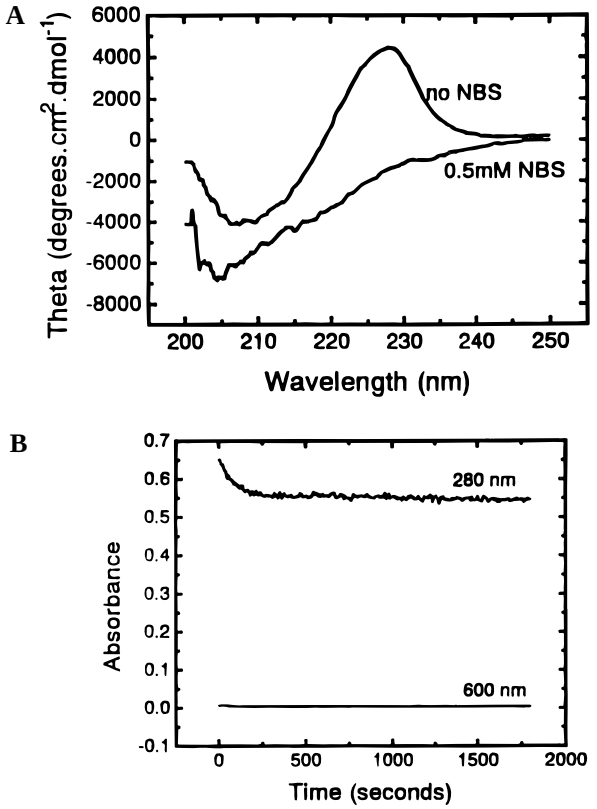

FIGURE 5: Modification of H6Sec13 tryptophans: (A) Far-UV CD spectra from 200 to 250 nm of purified H6Sec13 in 0.1 M sodium phosphate buffer, pH 7.0 at 25 °C, in the absence and presence of 0.5 mM NBS. (B) Absorbance of H6Sec13 in 0.1 M sodium phosphate buffer, pH 7.0, at 280 and 600 nm as a function of time following the addition of 0.5 mM NBS.

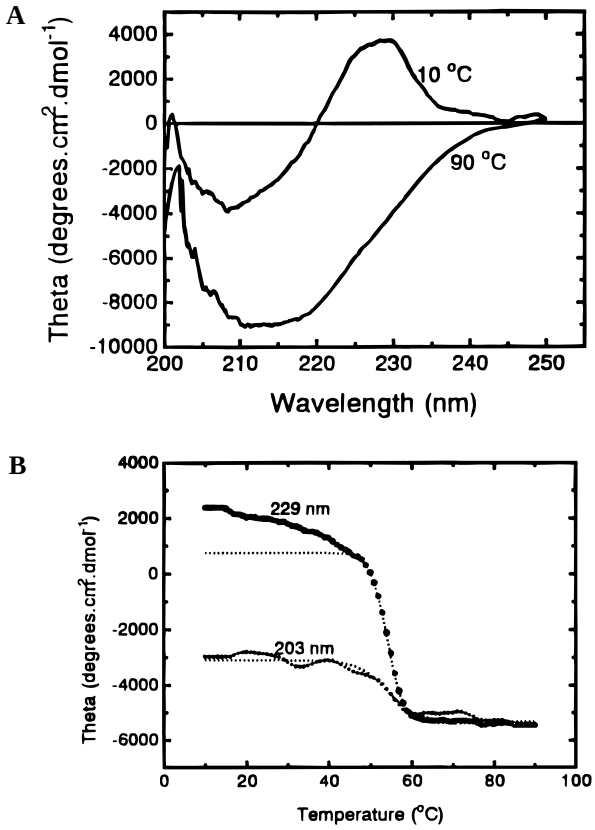

FIGURE 6: (A) Far-UV CD spectra from 200 to 250 nm of purified H6Sec13 in 50 mM Tris-HCl, pH 8.0. (B) Thermal denaturation curve of H6Sec13 in 50 mM Tris-HCl, pH 8.0, at 228.5 and 203.5 nm.

OD_{600} as a function of time (Figure 5B). No significant change in OD_{600} was observed in the time course of the reaction, indicating that the decrease in OD_{280} as a function of time is not due to H6Sec13 precipitation but due to tryptophan modification. The number of tryptophan residues modified (out of a total of 15) was found to be 6.3 ± 0.3 (SEM, $n = 3$).

The CD spectra of H6Sec13 at 10 °C and after heat denaturation at 90 °C are shown in Figure 6A. Heat denaturation at 90 °C abolished the positive molar ellipticity observed at 229 nm for native H6Sec13, indicating a disruption of the tertiary structure (Figure 6A). The thermal denaturation of H6Sec13 was irreversible. The thermal denaturation curve (molar ellipticity vs. temperature) of H6Sec13 at 229 nm shows a two-component denaturation curve (Figure 6B). There is an initial slow decline in ellipticity between 10 and 45 °C followed by a sharp cooperative melting curve (T_m = 54 °C) shown in dotted lines. The T_m is identical to that measured at 203 nm where we observe only one component of the curve. The shape of the curve and the T_m were the same as at 203 nm when measured at 210 and 217 nm (data not shown).

The Sec13 Model. The model of Sec13 suggests a compact structure that is made up of six WD repeats arranged in a propeller structure as shown in Figure 7A. The blades of the propeller formed by four slightly twisted antiparallel β-stands (a, b, c, and d) are organized around a central channel. Both the structure as a whole and the channel are wider at the end shown as the bottom in Figure 7B.

DISCUSSION

Sec13 belongs to a large family of proteins that are involved in a wide variety of functions (Neer et al., 1994). It is 24% identical and 48% similar to the sequence of rat $G_{\beta 1}$. These two proteins share a conserved sequence motif, the WD repeat, which occurs seven times in $G_{\beta 1}$ and six times in Sec13. WD repeats were predicted to fold into a structure composed of β-strands and turns (Neer et al., 1994). The newly available crystal structure of $G_{\beta 1}$ shows that the repeats do form such structures (Wall et al., 1995; Lambright et al., 1996; Sondek et al., 1996). The properties of H6Sec13 determined by biophysical and biochemical methods are consistent with those predicted from the model (Figure 7).

The model predicts that H6Sec13 would be completely resistant to digestion with trypsin, and we find H6Sec13 is not cleaved by trypsin digestion despite the presence of 29 potential tryptic cleavage sites. This behavior of H6Sec13 is very similar to that of native $G_{\beta 1}$ which has 32 potential tryptic cleavage sites but only one site (Arg 129) which is accessible to trypsin. In $G_{\beta 1}$, all the lysines and arginines are present either in the tight turns between the β-strands or within the β-strands themselves, and only Arg 129 is present on a large surface loop. Both the peptide bond (on the carboxyl side of Arg 129) and the side chain of Arg 129 of $G_{\beta 1}$ are exposed to the surface thereby creating a good site for trypsin cleavage. In our Sec13 model, with the exception of Lys 168, all the lysines and arginines are present in the tight turns and β-strands. Even though Lys 168 is present in the loop between "a" and "b" strands of repeat 4, the peptide bond on the carboxyl side of Lys 168 is not

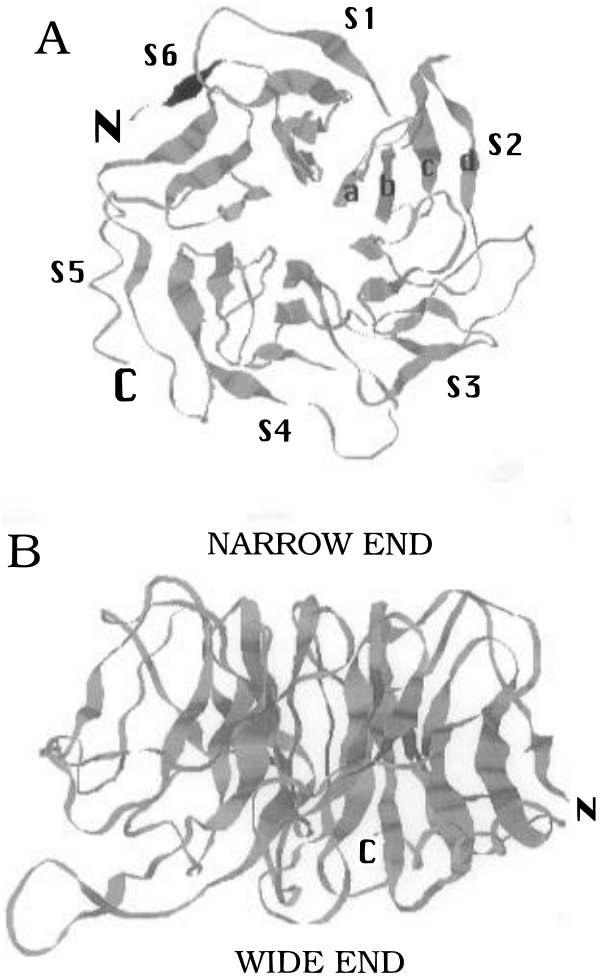

FIGURE 7: Overall predicted structure of Sec13. (A) Ribbon drawing viewed down the central tunnel showing the 6 WD repeats of Sec13 arranged in a β-propeller structure. β-Strands are labeled as a, b, c, and d; β-sheets are labeled as S1, S2 ..., S6. (B) Ribbon drawing of the side view of the Sec13 model.

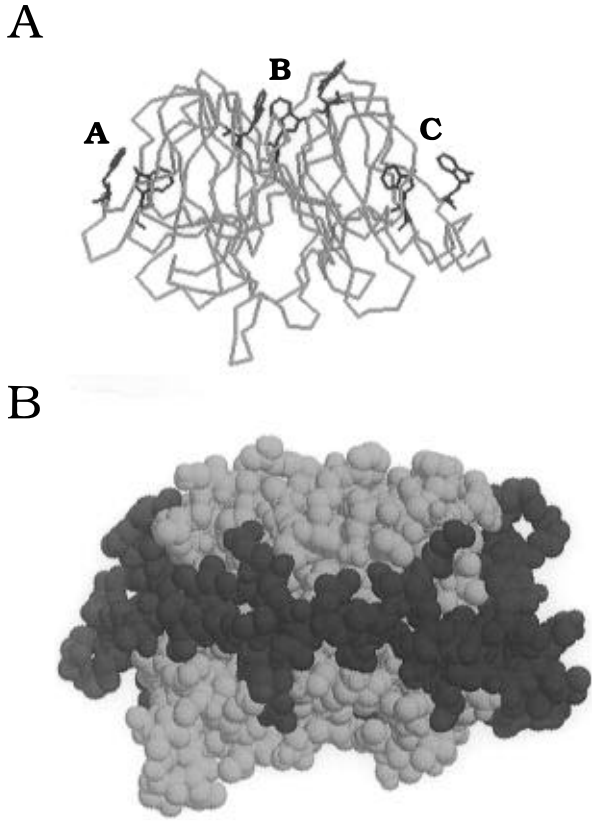

FIGURE 8: (A) Backbone structure of the side view of the Sec13 model with the surface tryptophans shown in ball-and-sticks. Cluster A, Trp 89 and Trp 82; cluster B, Trp 206, Trp 557, and Trp 258; and cluster C, Trp 234 and Trp 243. (B) Space-filling model of the side view of Sec13 highlighting the variable regions.

predicted to be exposed to the outer surface and therefore should be inaccessible to trypsin digestion.

The CD analysis of purified H6Sec13 at 25 °C predicts very little (less than 10%) α-helix. This is in accordance with our model of Sec13 which predicts primarily β-sheets and minimal α-helix. The CD spectrum for native Sec13 has an unusual positive ellipticity at 229 nm that has been attributed to disulfide bonds (Hider et al., 1988) and/or the interactions between aromatic residues (Woody, 1978). Interestingly, hemopexin, a non-WD repeat protein, which, like $G_{\beta 1}$, is known to form a β-propeller structure (Faber et al., 1995), also exhibits this positive ellipticity in the 230 nm region (Morgan & Muller-Eberhard, 1974). In hemopexin the positive maximum at 233 nm is due to the tryptophan residues. H6Sec13 contains three cysteines and fifteen tryptophans. Our data suggest that the positive ellipticity at 229 nm is most likely due to the tryptophan residues since the 229 nm maximum can be eliminated by modifying the tryptophans of native H6Sec13 with NBS. Out of fifteen tryptophans, 6.3 ± 0.3 (SEM, $n = 3$) tryptophan residues are modified under the conditions in which the positive ellipticity at 229 nm disappears. This suggests that there are two sets of tryptophans present in H6Sec13: those that are present on the surface of the molecule and can be modified by NBS and those that are inaccessible to NBS modification. Our model of Sec13 predicts two such sets of tryptophans (Figure 8A). There are at least seven tryptophans (arranged in three clusters) that are present on the surface of the molecule. Trp 89 and Trp 82 (cluster A) and Trp 243 and Trp 234 (cluster C) are present on the side surfaces of Sec13, whereas Trp 57, 206, and 258 (cluster B) are aligned around the central channel of the β-propeller. Hemopexin, which exhibits a positive maximum at 233 nm, shows two clusters of tryptophans on the surface of the molecule. In Sec13, the remaining eight tryptophans are buried inside in the molecule and would not be expected to be modified by NBS. In addition, our model predicts that the cysteines in Sec13 are widely separated and could not form disulfide bonds.

At 229 nm, the thermal denaturation curve of H6Sec13 is biphasic. The sharp denaturation of H6Sec13 ($T_m = 54$ °C) is due to the cooperative unfolding of the molecule. The identical T_m of 54 °C is observed when denaturation is followed at 203 nm which reflects the unfolding of the backbone. The cooperative denaturation is consistent with a tightly packed structure and similar to that determined by different means for G_β (Thomas et al., 1993). The slow noncooperative melting of H6Sec13 between 10 and 45 °C is probably due to increased side chain motion of the surface set of tryptophans.

According to the model, Sec13 assumes a compact β-propeller structure which is held together by a "velcro" provided by the outermost (d) strand in the last blade (Figure 7A). The sequence prior to the (a) strand of the first blade makes the (d) strand of the last blade, thereby closing the

ring. The blades of the propeller are organized around a central channel in such a way that the top surface is slightly narrower than the bottom surface (Figure 7B). In other β-propellers, the narrow surface interacts with various ligands, such as calcium ion in collagenase (Li et al., 1992); a heme in hemopexin (Faber et al., 1992); and a quinone in methanol dehydrogenase (Xia et al., 1992). In heterotrimeric G proteins, G_α occupies an equivalent position, sitting asymmetrically on the narrow surface of the G_β subunit (Wall et al., 1995; Lambright et al., 1996; Sondek et al., 1996). It is therefore quite likely that the narrow end (top) of Sec13 provides a surface for protein assembly. Mutations of the loops and turns on this surface are likely to disturb protein/protein association.

Sec13 associates with a 150 kDa protein (also a WD repeat protein) and forms a large complex (Pryer et al., 1993). The Sec13 complex, Sar-1 and Sec23p complex are the components of vesicle coat (Barlowe et al., 1994) and are required *in vitro* for the formation of transport vesicles that carry α-factor precursor from the endoplasmic reticulum to the Golgi apparatus (Pryer et al., 1993). At present, the exact structural or functional role of Sec13 in vesicular traffic is very poorly understood. The Sec13 model presented in this paper can act as a framework for the design of experiments to understand the role of Sec13 in vesicular budding. As discussed above, we speculate that the loops and turns in the narrow end of Sec13 are most likely involved in the interactions of Sec13 with the other proteins in the complex. More specifically, we propose that the large loop between the strands a and b of the fourth repeat (residues 155−171) has an important regulatory function. Furthermore, the variable regions of the WD repeats are attractive candidates for specific protein binding sites because they are the most different among all the members of the WD repeat family and because they are predicted to form a belt around the molecule (Figure 8B). The surface hydrophobicity plot of the Sec13 model does not indicate any large hydrophobic patches and therefore suggests that Sec13 does not interact with the lipid vesicles directly but via an intermediate protein.

The concordance of the model of Sec13 presented in this paper with the biochemical and biophysical studies suggests that this model can be useful as a guide to further experiments designed to elucidate the function of Sec13 in vesicular traffic.

REFERENCES

Barlowe, C., Orci, L., Yeung, T., Hosobuchi, M., Hamamoto, S., Salama, N., Rexach, M. F., Ravazzola, M., Amherdt, M., & Schekman, R. (1994) *Cell 77*, 895−907.

Brooks, B. R., Bruccoleri, R. E., Olafson, B. D., States, D. J., Swaminathan, S., & Karplus, M. (1983) *J. Comput. Chem. 4*, 187−217.

Chen, L., Mathews, F. S., Davidson, V. L., Huizinga, E. G., Vellieux, F. M. D., & Hol, W. G. J. (1992) *Proteins Struct., Funct., Genet. 14*, 288−299.

Faber, H. R., Groom, C. R., Baker, H. M., Morgan, W. T., Smith, A., & Baker, E. N. (1995) *Structure 3*, 551−559.

Fong, H. K., Hurley, J. B., Hopkins, R. S., Miake-Lye, R., Johnson, M. S., Doolittle, R. F., & Simon, M. I. (1986) *Proc. Natl. Acad. Sci. U.S.A. 83*, 2162−2166.

Garcia-Higuera, I., Fenoglio, J., Li, Y., Lewis, C., Panchenko, M. P., Reiner, O., Smith, T. F., & Neer, E. J. (1996) *Biochemistry* (in press).

Gill, S. C., & von Hippel, P. H. (1989) *Anal. Biochem. 182*, 319−326.

Greenfield, N., & Fasman, G. D. (1969) *Biochemistry 8*, 4108−4116.

Hider, R. C., Kupryszewski, G., Rekowski, P., & Lammek, B. (1988) *Biophys. Chem. 31*, 45−51.

Ito, N., Phillips, S. E. V., Yadav, K. D. S., & Knowles, P. F. (1994) *J. Mol. Biol. 238*, 794−814.

Janknecht, R., de Martynoff, G., Lou, J., Hipskind, R. A., Nordheim, A., & Stunnenberg, H. G. (1991) *Proc. Natl. Acad. Sci. U.S.A. 88*, 8972−8976.

Laemmli, U. K. (1970) *Nature 227*, 680−685.

Lambright, D. G., Sondek, J., Bohm, A., Skiba, N. P., Hamm, H. E., & Sigler, P. B. (1996) *Nature 379*, 311−319.

Li, J., Brick, P., O'Hare, M. C., Skarzynski, T., Lloyd, L. F., Curry, V. A., Clark, I. M., Bigg, H. F., Hazleman, B. L., Cawston, T. E., & Blow, D. M. (1995) *Structure 3*, 541−549.

Morgan, W. T., & Muller-Eberhard, U. (1974) *Enzyme 17*, 108−115.

Neer, E. J., & Smith T. F. (1996) *Cell 84*, 175−178.

Neer, E. J., Schmidt, C. J., Nambudripad, R., & Smith, T. F. (1994) *Nature 371*, 297−300.

Pryer, N. K., Salama, N. R., Schekman, R. W., & Kaiser, C. A. (1993) *J. Cell Biol. 120*, 865−875.

Ron, D., Chen, C.-H., Caldwell, J., Jamieson, L., Orr, E., & Mochly-Rosen, D. (1994) *Proc. Natl. Acad. Sci. U.S.A. 91*, 839−843.

Salama, N. R., Yeung, T., & Schekman, R. W. (1993) *EMBO J. 12*, 4073−4082.

Schmidt, C. J., & Neer, E. J. (1991) *J. Biol. Chem. 266*, 4538−4544.

Shaywitz, D. A., Orci, L., Ravazzola, M., Swaroop, A., & Kaiser, C. A. (1995) *J. Cell Biol. 128*, 769−777.

Sondek, J., Bohm, A., Lambright, D. G., Hamm, H. E., & Sigler, P. B. (1996) *Nature 379*, 369−374.

Spande. T. F., & Witkop, B. (1967) *Methods Enzymol. 11*, 498−506.

Surles, M. C. (1992) *Computer Graphics 26*, 221−230.

Swaroop, A., Yang-Feng, T. L., Liu, W., Gieser. L., Barrow, L. L., Chen, K.-C., Agarwal, N., Meisler, M. H., & Smith, D. I. (1994) *Hum. Mol. Genet. 3*, 1281−1286.

Thomas, T. C., Sladek, T., Yi, F., Smith, T., & Neer, E. J. (1993) *Biochemistry, 32*, 8628−8635.

Wall, M. A., Coleman, D. E., Lee, E., Iniguez-Lluhi, J. A., Posner, B. A., Gilman, A. G., & Sprang, S. R. (1995) *Cell 83*, 1047−1058.

Woody, R. W. (1978) *Biopolymers 17*, 1451−1467.

Xia, Z.-X., Dai, W.-W., Xiong, J.-P., & Hao, Z.-P., Davidson V. L., White S., & Mathews F. S. (1992) *J. Biol. Chem. 267*, 22289−22297.

BI961616X